# Universal Properties of Ferroelectric Domains

Igor A. Luk'yanchuk,[1,2] Laurent Lahoche,[3] and Anaïs Sené[1]
[1]*Laboratory of Condensed Matter Physics, University of Picardie Jules Verne, Amiens, 80039, France*
[2]*L. D. Landau Institute for Theoretical Physics, Moscow, Russia*
[3]*Roberval Laboratory, University of Technology of Compiegne, France*
(Received 22 February 2008; published 9 April 2009)

Based on the Ginzburg-Landau approach, we generalize the Kittel theory and derive the interpolation formula for the temperature evolution of a multidomain polarization profile $\mathbf{P}(x, z)$. We resolve the long-standing problem of the near-surface polarization behavior in ferroelectric domains and demonstrate polarization vanishing instead of the usually assumed fractal domain branching. We propose an effective scaling approach to compare the properties of different domain-containing ferroelectric plates and films.

DOI: 10.1103/PhysRevLett.102.147601 PACS numbers: 77.80.Bh, 77.55.+f, 77.80.Dj

The design of ferroelectric devices necessitates taking into account such finite size effects as the formation of polarization-induced surface charges that, in turn, produce the energy consuming electrostatic depolarizing fields (see Ref. [1] for review). As a result, regular periodic structures of 180° domains that alternate the surface charge distribution, first proposed by Landau and Lifshitz [2,3] and by Kittel [4] for ferromagnetic systems, can be formed in uniaxial easy-axis (natural or stress-induced) ferroelectric plates or films as an effective mechanism to confine the depolarization field to the near-surface layer and reduce its energy [Fig. 1(a)]. The energy balance between the field-penetration depth ($\sim$ domain width $d$) and domain wall (DW) concentration ($\sim d^{-1}$) leads to the famous square-root Kittel dependence of $d$ on the film thickness $2a_f$ [4–7]:

$$d = \sqrt{\gamma(\epsilon_\perp/\epsilon_\parallel)^{1/2}(2a_f\xi_{0x})}, \qquad \gamma = \frac{2\sqrt{2}\pi^3}{21\zeta(3)} \simeq 3.53, \tag{1}$$

where $\epsilon_\parallel$ and $\epsilon_\perp$ are the longitudinal and transversal dielectric constants and $\xi_{0x}$ is the transverse coherence length (roughly equal to the DW thickness).

Consider the standard geometry [5] when the uniaxial ferroelectric film is sandwiched by electroded paraelectric passive layers of width $a_p$ and permittivity $\varepsilon_p$. The multidomain state should exist in certain intervals of film thickness $2a_f$ as shown in the phase diagram in Fig. 1(c) and defined by the condition that delineates the applicability of Eq. (1) and of our further consideration:

$$\xi_{0x} < d(2a_f) < a_p \tag{2}$$

the dependence $d(2a_f)$ being given by (1). We also assume the most realistic case $\varepsilon_p \ll \varepsilon_\perp < \varepsilon_\parallel$ that gives $d \ll a_f$. At this stage, the properties of domain structure do not depend on $a_p$, $\varepsilon_p$, and electrodes. For thicker films, when $d(2a_f)$ approaches to $a_p$, the emergent depolarizing field interacts with screening electrodes, Eq. (1) is no longer valid, $d$ grows exponentially with $a_p^{-2}$ , and domains practically emerge from the sample. However, in free standing electrodeless sample ($a_p \to \infty$), Kittel domains can exist in a wider interval of $2a_f$ unless another restricting mechanism of the internal free charges screening does not came into the play. For thinner films, we are turning to the region of little-studied atomic-size (microscopic) domains [8].

While domain structures should play a crucial role in the properties of thin ferroelectric films, only a few theoretical analytical studies of their temperature dependence have been performed. In particular, the mostly used Kittel ap-

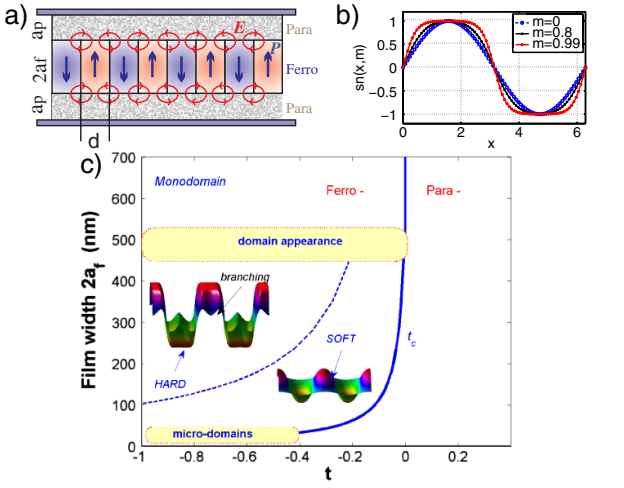


FIG. 1 (color online). (a) Multidomain texture of ferroelectric polarization in uniaxial ferroelectric film, sandwiched by two paraelectric (dead) layers. The emerging depolarization electric field is provided by alternating polarization-induced surface charges and confined in the near-surface layer of thickness, comparable with domain width $d$. (b) Elliptical functions $y = \mathrm{sn}(x, m)$ for different parameters $m$ that we use to model the domain profile at different $t$. (c) Phase diagram of domain states as function of sample thickness $2a_f$ and reduced critical temperature $t = T/T_{c0} - 1$. Polarization profiles of hard and soft domains were obtained by numerical solution of Eqs. (6)–(9). We assume that $\varkappa_\parallel \simeq 500$, $\varepsilon_\perp \simeq 100$, $\varepsilon_p \ll \varepsilon_\perp, \varkappa_\parallel$, $\xi_{0x} \simeq 1$ nm, and $a_p \simeq 30$ nm.

 

proach [3–5] in which the domain texture is considered as a set of up- and down-oriented (hard) domains, having a flat polarization profile $\mathbf{P}(x, z) = \pm P_0$ (DW supposed to be infinitely thin and boundary effects on the ferroelectric-paraelectric interface neglected), is valid only far below the transition temperature $T_c$. Although the more general consideration, proposed by Chensky and Tarasenko (CT) [9] (see also [6,10]) and based on Ginzburg-Landau equations coupled with electrostatic equations is valid in the whole temperature interval, only the solution close to $T_c$ was found.

It is the objective of the present Letter to establish the approach that permits to model the temperature evolution of domain structure. Basing on CT equations, we derive the analytical expression (19) for domain polarization profile that is valid in the whole temperature interval and includes the Kittel (at low $T$) and CT (at $T = T_c$) solutions as particular cases. Then, we deduce universal scaling relations between parameters of the multidomain state that should be useful in treatment of experimental data. Our approach is complimentary to the frequently used first-principia simulations (see, e.g., [11]), that reproduce the domain structure but give no general vision and parameter dependence of the results.

To deduce the CT equations, we are basing on the Euler-Lagrange variational formalism that permits also to obtain the correct boundary conditions as variation of surface terms. The generating energy functional is written as [3]

$$F = \int \tilde{\Phi}(\mathbf{P}, \mathbf{E}) dx dz, \qquad \tilde{\Phi}(\mathbf{P}, \mathbf{E}) = \tilde{\Phi}(\mathbf{P}, 0) - \mathbf{E}\mathbf{P} - \frac{1}{8\pi}\mathbf{E}^2 \tag{3}$$

where $\mathbf{E} = (E_x, E_z)$, $\mathbf{P} = (P_x, P_z)$ and the field-independent part

$$\tilde{\Phi}(\mathbf{P}, 0) = \frac{4\pi}{\varepsilon_\perp}\frac{1}{2}P_x^2 + \frac{4\pi}{\varepsilon_{i\|}}\frac{1}{2}P_{zi}^2 + \frac{4\pi}{\varkappa_\|} f(P) \tag{4}$$

includes the transversal $P_x$, and nonpolar longitudinal $P_{zi}$ noncritical contributions ($\varepsilon_\perp$, $\varepsilon_{i\|} \gg 1$). The nonlinear Ginzburg-Landau energy depends on the spontaneous $z$-oriented polarization $P$ (assuming that $P_z = P_{zi} + P$) and is written as

$$f(P) = \frac{t}{2}P^2 + \frac{1}{4}P_0^{-2}P^4 + \frac{\xi_{0x}^2}{2}(\partial_x P)^2 + \frac{\xi_{0z}^2}{2}(\partial_z P)^2 \tag{5}$$

where the reduced temperature $t$ is expressed via the bulk critical temperature as: $t = T/T_{c0} - 1$, parameter $\varkappa_\|$ is expressed via paraelectric Curie constant $C$, and via longitudinal zero-temperature permittivity $\varepsilon_\|$ in (1) as: $\varkappa_\| = C/T_{c0} \simeq 2\varepsilon_\|$, and coefficient $P_0$ is roughly equal to the saturated bulk polarization at $T \ll T_c$.

The variation of (3) with respect to $P$ and the electrostatic potential $\varphi$ ($\mathbf{E} = -\nabla\varphi$) and excluding of the non-essential variables $P_x$ and $P_{zi}$ gives the system of required equations that describe the ferroelectric transition taking into account the depolarizing field:

$$\begin{gathered}(t - \xi_{0x}^2\partial_x^2 - \xi_{0z}^2\partial_z^2)P + (P/P_0)^2 P = -\frac{\varkappa_\|}{4\pi}\partial_z\varphi, \\ (\varepsilon_{i\|}\partial_z^2 + \varepsilon_\perp\partial_x^2)\varphi = 4\pi\partial_z P.\end{gathered} \tag{6}$$

These equations should be completed by the Poisson equation for paraelectric media in which ferroelectric film is embedded:

$$(\partial_z^2 + \partial_x^2)\varphi^{(p)} = 0, \tag{7}$$

and by boundary conditions at the Para-Ferro interface

$$\varepsilon_{i\|}\partial_z\varphi - \varepsilon_p\partial_z\varphi^{(p)} = 4\pi P, \qquad \varphi = \varphi^{(p)}, \qquad \partial_z P = 0 \tag{8}$$

that are also obtained as result of variation of (3) [12]. Periodic conditions

$$P(x, z) = P(x + 2d, z) \qquad \varphi(x, z) = \varphi(x + 2d, z) \tag{9}$$

with variational parameter $d$ are imposed to describe the periodicity of domain structure.

A simplification can be achieved if we present the initial functional (3) using the dimensionless (prime) variables

$$\begin{gathered}z = a_f z', \qquad x = \tau^{-1/2}\xi_{0x}x', \qquad t = \tau t', \qquad P = \tau^{1/2}P_0 P', \\ \varphi = \frac{1}{\varkappa_\|}\tau^{3/2}a_f P_0\varphi', \qquad F = \frac{a_f\xi_{0x}}{\varkappa_\|}\tau^{3/2}P_0^2 F'\end{gathered} \tag{10}$$

with

$$\tau = \left(\frac{\varkappa_\|}{\varepsilon_\perp}\right)^{1/2}\frac{\xi_{0x}}{a_f} \ll 1 \tag{11}$$

in truncated form,

$$\begin{aligned}F' = \int\Bigg[&4\pi\left(\frac{1}{2}t'P'^2 + \frac{1}{4}P'^4 + \frac{1}{2}(\partial_x' P')^2\right) \\ &- \frac{1}{8\pi}(\partial_x'\varphi')^2 + P'\partial_z'\varphi'\Bigg]dx'dz'\end{aligned} \tag{12}$$

that was obtained after neglecting the small terms

$$\hat{A}_1 = \left(\frac{\varepsilon_\perp}{\varkappa_\|}\right)^{1/2}\frac{\xi_{0z}}{a_f}(\partial_z' P')^2, \quad \hat{A}_2 = \frac{\varepsilon_{i\|}}{\varkappa_\|}\left(\frac{\varkappa_\|}{\varepsilon_\perp}\right)^{1/2}\frac{\xi_{0x}}{a_f}(\partial_z'\varphi')^2 \tag{13}$$

(justification is given in [13]) and minimizing over $P_x$, $P_{zi}$.

The Euler-Lagrange variation of (12) over $P'$ and $\varphi'$ gives the corresponding dimensionless equations

$$(t' - \partial_x'^2)P' + P'^3 = -\frac{1}{4\pi}\partial_z'\varphi', \tag{14}$$

$$\partial_x'^2\varphi' = 4\pi\partial_z' P', \tag{15}$$

and boundary conditions at $z'_- = 0$ and at $z'_+ = 2a'_f = 2$

$$P' = 0, \qquad \varphi' = \varphi'^{(p)}. \tag{16}$$

that are simpler then conditions (8) since the order of (6) was reduced by neglecting (13). We stress here that these

conditions are *derived* from functional (12) as variational surface terms.

Passage to dimensionless variables is the powerful tool that permits to study the various properties of ferroelectric domains even without solution the differential equations. Note first that Eqs. (14) and (15) contain only one driving variable—the dimensionless temperature $t'$. Therefore, the "master" temperature dependence of any physical parameter calculated from (14) and (15) can be rescaled for any other ferroelectric sample, using the relations (10).

We derive now such "master" variational solution of Eqs. (14) and (15) for domain profile $P'(x', z', t')$ valid in the whole temperature interval. Note first that these equations can be solved analytically close to the transition to a multidomain ferroelectric state [9,10] that occurs at

$$t_c' = -\pi, \qquad t_c = -2\pi\sqrt{\frac{\varkappa_\parallel}{\varepsilon_\perp}}\frac{\xi_{0x}}{2a_f} \tag{17}$$

(in dimensionless and dimensional variables), when polarization has the sinusoidal (soft) distribution

$$P'(x', z') = A(t')\sin\frac{\pi x'}{d_c'}\sin\pi z' \tag{18}$$

with the half-period $d_c' = \sqrt{2\pi}$ (that is expressed as (1) in dimensional variables but with $\gamma = \pi$ and $\epsilon_\parallel = \varkappa_\parallel/2$). At lower temperatures, domain walls become sharper due to the admixture of higher harmonics. At lower temperatures, the domains recover the (hard) Kittel-like profile.

To account for both these cases by the unique interpolation formula, we shall exploit the periodical elliptical sinus function $y = \mathrm{sn}(x, m) = \mathrm{sn}(x + 4K, m)$ depicted in Fig. 1(b), frequently used to describe the incommensurate phases [14]. The $1/4$ of the elliptical sinus period is given by the tabled first kind elliptical integral $K(m)$ [15]. The useful property of $\mathrm{sn}(x, m)$ is that, depending on the parameter $0 < m < 1$, it recovers the all described above domain regimes: from the soft one (18) at $m = 0$ when $\mathrm{sn}(x, m) \to \sin x$ [like in Eq. (18)] to the hard (Kittel-like) one at $m \sim 1$ when $\mathrm{sn}(x, m) \to$ stepwise function.

After some algebra [13], we arrive to the following variational expression

$$P' = A(t')\mathrm{sn}\left[\frac{4K_1(t')}{2d'(t')}x', m_1(t')\right]\mathrm{sn}[K_2(t')z', m_2(t')] \tag{19}$$

where the temperature dependencies of parameters $m_1(t)$ and $m_2(t)$, elliptic integrals $K_1(t)$ and $K_2(t)$, amplitude $A(t)$, and domain lattice half-period $d(t)$ are presented in Fig. 2 and for practical use are approximated as

$$\begin{aligned} &A'(t') \simeq \sqrt{t'\tanh 0.35(t' - t_c')}, \qquad d'(t') \simeq 2.6 \\ &K_{12}(t') \simeq 0.85\sqrt{-t'}, \qquad m_{12}(t') \simeq \tanh 0.27(t_c' - t'). \end{aligned} \tag{20}$$

Formula (19) satisfies the boundary conditions

$$P'(x', z') = P'(x' + 2d', z'), \qquad P'(x', 0) = P'(x', 2) = 0, \tag{21}$$

recovers the soft domain structure (18) at $t_c'$ when $m_{12}(t_c') = 0$, $A(t') \sim (t_c' - t')^{1/2}$ and the Kittel-like structure at low $t_c'$ when $m_{12}(t_c') \to 1$, $A(t') \simeq (-t')^{1/2}$, and gives the domain profile at arbitrary $t'$. Parameters $K_{12}(t')$ determine the space scale of polarization variation: in dimensional variables, the characteristic domain wall thickness is $\xi_x(t) = \xi_{0x}/(-t)^{1/2}$ whereas the thickness of the near-surface layer where $P(z)$ restores its equilibrium value is $\sim d/(-t)^{1/2} \cdot (\varkappa_\parallel/\epsilon_\perp)^{1/2}$ (i.e., $\sim d$ at low $t$).

Variation and vanishing of polarization at the sample surface modifies the initial assumption of the Kittel model that polarization is permanent inside domain and resolves the long-standing paradox [3,16] according to which the permanent domain polarization should be reoriented close to sample surface by its own depolarization field that exists in the near-surface layer.

As it follows from our calculations, the nonuniform distribution of polarization pumps the depolarization charge $\rho(r) \sim \mathrm{div}\mathbf{P}$ from the sample surface inside the near-surface layer $\sim d$, reducing the unfavorable depolarization field [13] and its energy $\mathcal{E}_d \sim E^2/4\pi \sim 4\pi P^2$. The price of this—the dumping of the condensation energy $\mathcal{E}_c \sim 4\pi P^2/\epsilon_\parallel$—is not so high because $\epsilon_\parallel \gg 1$. That is why we believe that the near-surface polarization vanishing is a more effective mechanism to overcome the Kittel paradox in ferroelectrics and reduce the near-surface depolarization energy than the usually assumed [3,16] but rarely observed fractal branching of alternatively oriented permanent-polarization domains near the sample surface.

Polarization decay at the surface is the consequence of the boundary condition $P' = 0$ of simplified Eqs. (14)–(16). The validity of this effect is illustrated in Fig. 3 where we compare the numerical solution of simplified Eqs. (14)–(16) [Fig. 3(b)] with that for the complete set of CT equations [Fig. 3(a)]. Clearly, the tendency of polarization

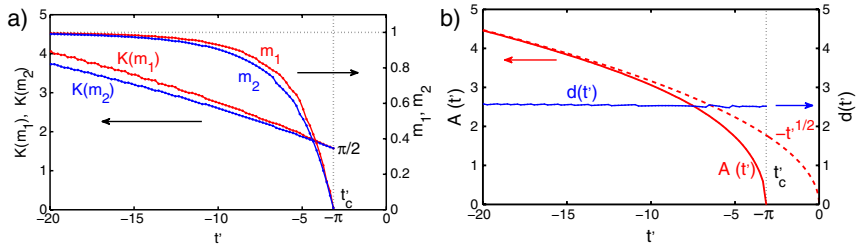


FIG. 2 (color online). Temperature dependencies of parameters of Eq. (19): (a) elliptic arguments $m_1$ and $m_2$, elliptic integrals $K_1$ and $K_2$, (b) domain amplitude $A$ and domain lattice period $d'$. All the variables are dimensionless.

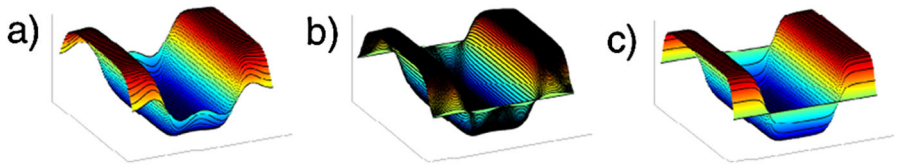


FIG. 3 (color online). Polarization of Kittel domain. (a) Numerical solution of complete CT Eqs. (6)–(9). (b) Numerical solution of simplified Eqs. (14)–(16). (c) Interpolation formula (19).

vanishing is conserved for the case of general solution in Fig. 3(a), although the "real" boundary condition $\partial_z P = 0$ (8) is satisfied exactly at the surface. Interesting to note that the precursor of the competitive surface domain branching is also seen at Figs. 3(a) and 3(b) as ripples at the domain endpoints. The corresponding variational solution (19) at Fig. 3(c) is more smooth, but correctly represents the properties of numerical profile.

We present now several remarkable conclusions about the physical properties of the multidomain state which can be obtained only from the scaling properties (10), without solution of CT Eqs. (6)–(9). (i) Any transverse length parameter scales as $\tau^{-1/2}\xi_{0x}$. This, in particular, justifies the Kittel formula (1) for the domain width $d$ even beyond the flat domain approximation. A convincing demonstration of the validity of this scaling law was reported recently for various ferroelectric and ferromagnetic materials [7]. The temperature dependence $d(t)$ can be incorporated into (1) as dependence $\gamma = \gamma(t)$. Meanwhile, the results shown in Fig. 2(b) as well as finite-element simulations [6] indicate that the dependence $d(t)$ is very weak, and hence, one can extend the parameter $\gamma \simeq 3.53$ from (1) to any temperature. This, in particular, implies the low temperature hysteresis related with motion of DW. (ii) The temperature $t$ scales as $\tau$. Thus, to compare the domain-provided physical properties of different plates or films (even constructed from different materials), it should be instructive to trace their temperature dependencies using the rescaled coordinate $t/\tau$. (iii) All the domain-related properties and, in particular, the transition temperature $t_c$ (17) and the soft-to-hard domain crossover temperature $t^* \sim 10t_c$ scale as $1/2a_f$ with plate (film) width, as illustrated in Fig. 1(c). The temperature interval for the existence of soft-domains $\Delta t = t_c - t^*$ growth dramatically with decreasing film thickness and one can expect that for thin films with $2a_f <$ 100 nm, only soft domains with a gradual polarization distribution are possible.

Summarizing, we conclude that domains in *any* ferroelectric sample and at *any* temperature can be easily obtained from interpolation formulas (19) and (20) applying the scaling relations (10). This can be especially helpful to treat the experimental data, involving the local field distribution of polarization inside domains like ESR or Raman spectroscopy, TEM domain imagery, etc.

We demonstrated that depending on the temperature and sample width, domains can have soft (gradual) or hard (Kittel) profile. In any case, polarization has the tendency to vanish at sample surface.

Basing on universal scaling relations (10), we have demonstrated how the physical properties of the different multidomain films can be compared and mapped onto each other. We hope that such method will give the power tool for analysis and systematization of numerous experimental data for thin ferroelectric films.

This work was supported by the Region of Picardy, France, by STREP "Multiceral"(NMP3-CT-2006-032616) and by FP7 IRSES program "Robocon." We thank to Professor M. G. Karkut for useful discussions.

[1] M. Dawber, K. M. Rabe, and J. F. Scott, Rev. Mod. Phys. **77**, 1083 (2005).
[2] L. D. Landau and E. M. Lifshitz, Phys. Z. Sowjetunion **8**, 153 (1935).
[3] L. D. Landau and E. M. Lifshitz, *Electrodynamics of Continuous Media* (Elsevier, New York, 1985).
[4] C. Kittel, Phys. Rev. **70**, 965 (1946).
[5] A. M. Bratkovsky and A. P. Levanyuk, Phys. Rev. Lett. **84**, 3177 (2000).
[6] F. De Guerville, I. Lukyanchuk, L. Lahoche, and M. El Marssi, Mater. Sci. Eng. B **120**, 16 (2005).
[7] G. Catalan, J. F. Scott, A. Schilling, and J. M. Gregg, J. Phys. Condens. Matter **19**, 022201 (2007).
[8] A. M. Bratkovsky and A. P. Levanyuk, Integr. Ferroelectr. **84**, 3 (2006).
[9] E. V. Chensky and V. V. Tarasenko, Zh. Eksp. Teor. Fiz. **83**, 1089 (1982) [Sov. Phys. JETP **56**, 618 (1982)].
[10] V. A. Stephanovich, I. A. Luk'yanchuk, and M. G. Karkut, Phys. Rev. Lett. **94**, 047601 (2005).
[11] Bo-Kuai Lai, I. Ponomareva, and I. I. Naumov *et al.*, Phys. Rev. Lett. **96**, 137602 (2006).
[12] Frequently used more general boundary condition $\partial_z P = \lambda^{-1} P$ is obtained when polarization is constrained by additional surface contribution $\sim\lambda^{-1}\int P^2 dx$ to free energy (3). We neglect this term here.
[13] See EPAPS Document No. E-PRLTAO-102-016917 for technical derivation of (i) simplified equations and corresponding boundary conditions from the generating Euler-Lagrange functional, (ii) interpolation formula for domain polarization, (iii) justification of simplification of generating functional. For more information on EPAPS, see http://www.aip.org/pubservs/epaps.html.
[14] D. G. Sannikov, in *Incommensurete Phases in Dielectrics I. Fundamentals*, edited by R. Blinc and A. P. Levanyuk (Elsevier. Sci. Publ., Amsterdam, 1986), p. 43.
[15] *Handbook of Mathematical Functions*, edited by M. Abramowitz and I. A. Stegun (NBS, Washington, 1972), 10th ed.
[16] B. A. Strukov and A. P. Levanyuk, *Ferroelectric Phenomena in Crystals* (Springer, Berlin, 1998).